AD-A163 845 COMPARISON OF MEASURED AND COMPUTED BOUNDARY LAYERS AT THE TAIL-END OF TW..(U) ADMIRALTY MARINE TECHNOLOGY ESTABLISHMENT TEDDINGTON (ENGLAND.. G J COOPER JUN 85 1/1

UNCLASSIFIED AMTE(N)TM84063 DRIC-BR-97645 F/G 20/4 NL

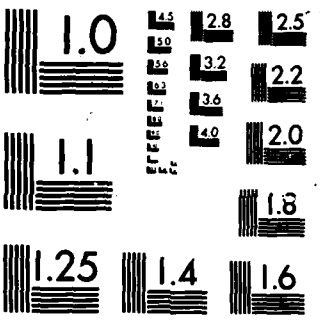

TECH MEMO AMTE(N) TM84063

COPY No. 14

AMTE(N)TM84063

ADMIRALTY RESEARCH ESTABLISHMENT (MARINE TECHNOLOGY)

COMPARISON OF MEASURED AND COMPUTED BOUNDARY LAYERS AT THE TAIL-END OF TWO AXISYMMETRIC BODIES IN THE A.R.E. QUIET WIND TUNNEL

G. J. COOPER

ARE (Teddington)
Queen's Rd TEDDINGTON
Middlesex TW11 0LN

JUNE 1985

2

AMTE(N)TM84063

COMPARISON OF MEASURED AND COMPUTED BOUNDARY LAYERS AT THE TAIL-END OF TWO AXISYMMETRIC BODIES IN THE ARE QUIET WIND TUNNEL

By

G J Cooper

Summary

This report shows comparisons of velocity profiles measured at the tail end of two axisymmetric bodies with velocity profiles produced by a potential flow and first order boundary layer computer model. The computer program can produce excellent agreement with measured data if the boundary layer transition position can be optimised in the computation.

This program will be a valuable aid to determining the model and duct configuration most suitable for simulating a particular full scale situation although some preliminary testing of models may be necessary to establish the actual boundary layer transition position and to change it using a boundary layer trip device or to optimise the position selected for the computation.

51 Pages
9 Figures

ARE(Teddington)
Queen's Road
TEDDINGTON, Middx TW11 OLN

June 1985

UNLIMITED

CONTENTS

INTRODUCTION

Wind tunnels are used for the testing of models of underwater vehicles because of the cheapness of the model and the reduced practical difficulties compared to similar experiments in water. However, low speed wind tunnel tests often result in the Reynolds number being an order of magnitude or more lower than the full scale situation it is intended to simulate. This difficulty may be partially overcome for studies of the flow around the tail and aft control surfaces of submarines and weapons by making the boundary layer profile and thickness (relative to some dimension such as hull radius) the same in the model test as in the full scale case. Geometrical changes can then be made and the effects on the flow assessed.

A computer model which calculates the potential flow and a first order boundary layer over an axisymmetric body in an open jet emerging from a duct was validated by comparisons of computed results with measurements made using two models in a small wind tunnel. The larger of the two models was found to be too large for the flow to develop fully. As a result, and because the computer model is to be applied to tests in the new ARE Quiet Wind Tunnel, further tests were carried out using this facility.

2. APPARATUS AND TEST CONDITIONS

The Quiet Wind Tunnel (figure 1) is of the straight through type with an air jet exhausting from 18 inch (0.457m) diameter ducting inside a working chamber with overall dimensions of 4m by 4m by 3m high. The length of ducting is variable and for these tests a length of 4 ft (1.22m) was used. Two wooden axisymmetric bodies were tested, each supported by a faired strut from a rail on the working chamber floor as illustrated in figure 2, the position being adjusted by moving the strut along the floor rail. The models are referred to by their diameters of 6 inches (0.152m), and 8 inches (0.203m) and their profiles are given in Table 1, although the actual models were truncated by the tail support strut.

Flow speeds within the boundary layer were measured with a constant temperature hot-wire anemometer, the probe having a single wire perpendicular to the probe axis. The probe was positioned so that traverses perpendicular to, and at the height of the body axis could be made. With the wire vertical and the probe axis parallel to the body axis the flow approached the wire at various angles of pitch depending on the probe position and the boundary layer profile, thus taking advantage of the probe's nominally flat response. The probe manufacturer's data showed that at an airspeed of 40 m/s a pitch angle of 30° causes a measurement error of less than 1%. This was considered sufficiently accurate for the purposes of this experiment and eliminated the need to calibrate the probe's directional response.

The hot-wire probe output voltage was calibrated against airspeed measured by a pitot-static probe by placing both probes at the same radial distance and just within the duct so that the flow velocity was well defined and the same for both positions.

Both probes were mounted on an optical bench so that they could be moved together to whatever axial position was required for the measurement of the boundary layer profile. The hot-wire probe was traversed through the boundary layer from the model's surface to a position close to the pitot-static probe so that the airspeeds measured by the two probes could be compared and the variability of the hot-wire measurements assessed. Voltages output by the hot-wire anemometer and the differential pressure transducer to which the pitot-static probe was connected were measured and processed by a data logger controlled by a desktop computer.

An investigation of the flow around the 6 inch diameter body had already been made by Cooper [1] in a small wind tunnel with a 12 inch (0.305m) diameter duct outlet or a 10 inch (0.267m) diameter convergent nozzle, the computed and measured results agreeing best for a model position approximately 18 inches (0.457m) into the duct or nozzle. Therefore, only a model position 18 inches into the duct was tested in the Quiet Wind Tunnel at an airspeed of 45 m/s.

The 8 inch diameter body was too large for use in the small wind tunnel and so three model positions were tested in the Quiet Wind Tunnel: 10 inches, 20 inches and 30 inches into the ducting, at a freestream airspeed of 45 m/s,giving a Reynolds Number of 3.3×10^6 based on the overall length. Airspeed profiles perpendicular to the body axis were made at several positions downstream of the duct for each model position. A pressure coefficient value was calculated for each speed measurement for comparison with the computed values from:

$$Cp = 1 - \left[\frac{Um}{U_o}\right]^2 \qquad (1)$$

where Um = the measured airspeed
and Uo = the freestream airspeed
although only the value at the boundary layer edge has any significance here.

3. COMPUTER MODEL

The method used to calculate the potential flow field is based on the surface singularity technique of Hess and Smith [2] and is described in full by Erith [3]. The axisymmetric body is represented by an axial distribution of ring sources over its surface, and the duct and jet boundaries by distributions of ring vortices. The onset flow is assumed to be uniform at upstream infinity and the boundary conditions applied are those of zero normal velocity on the body surface and zero tangential velocity outside the duct (there being no normal velocity) and outside the free jet boundaries. In addition the free jet boundary is a surface of constant pressure. The shape of this boundary is not known in advance, but must be determined as part of the solution. Hence an iterative procedure is necessary, in which an initial estimate is made of the jet boundary shape. The source and vortex strengths are then determined by applying the remaining boundary conditions, and the flow field is computed. If the assumed jet boundary shape does not coincide with a streamline of the flow then an adjustment must be made and the computation repeated. After convergence has been attained (generally in less

than 10 iterations) the potential flow calculation is complete and the program proceeds to the calculation of the boundary layer on the body surface.

The boundary layer computation is a first order one, ignoring any effect of the boundary layer on the potential flow. Furthermore the boundary layer on the inner surface of the duct is neglected. The laminar portion of the boundary layer, from the front stagnation point to a prescribed transition position is dealt with by the integral method of Pohlhausen [4]. The turbulent boundary layer, which is of particular interest here, is calculated by the method of Myring [5], in which a momentum integral equation and an equation involving the rate of entrainment of the fluid into the boundary layer are integrated along the body surface. Solution of this pair of simultaneous equations enables momentum area and a normalised shape parameter to be obtained for the boundary layer at positions along the body, and all other boundary layer parameters are obtained from these.

Input to the computer program consists of nozzle and body coordinates, an initial estimate of the jet edge coordinates, the position of the boundary layer transition from laminar to turbulent flow and the Reynolds number. The output gives the potential flow velocity profiles and boundary layer parameters at selected positions along the body from which the boundary layer profiles were calculated.

4. DATA PROCESSING

A program was written for the computer control of the data logger and to calculate the flow velocity components from each set of measurements. The output from the program gave the position of the probe in terms of the axial distance aft of the model's nose and the radial distance from the model's axis, the freestream airspeed obtained from the wind tunnel console, the airspeeds measured by the pitot-static and hot-wire probes and the calculated pressure coefficient. After each traverse the d.c.and r.m.s. voltages from the hot-wire probe were listed, together with a temperature compensation factor and the air density so that computed speeds could be checked if necessary.

Inspection of the data showed that the airspeed measured by the hot-wire probe when close to the pitot-static probe was usually less than that measured by the pitot-static probe. This discrepancy was probably due to inaccurate compensation for ambient temperature drift resulting from the lag of the temperature sensor near the roof of the working chamber relative to the changes in air jet temperature, and to contamination of the hot-wire element by dirt particles carried in the airflow. For the purposes of this experiment a single factor was applied to the speeds of each velocity profile measured by the hot-wire probe in order to get agreement with the pitot-static probe measurement. It is recommended that in future experiments temperature compensation be made either analytically as for this experiment but using a measurement of the air jet temperature, or by adjusting the d.c. balance of the anemometer bridge before every measurement. Contamination of the wire will have to be removed frequently by dipping the probe in acetone.

The adjusted values of speed measured by the hot-wire probe were plotted against radial distance for comparison with computed values of the potential flow and the first order boundary layer profile. The resultant velocity of the potential flow was calculated from values of the axial and radial components tabulated by the program, but the boundary layer profiles had to be calculated from the values of boundary layer thickness, δ, and displacement thickness, δ^*, given by the program. It was assumed that the boundary layer profile was of the form;

$$\frac{U}{U_1} = \left(\frac{y}{\delta}\right)^{1/n} \qquad (2)$$

where U is the flow velocity in the boundary layer at distance y from the body surface and U_1 is the velocity at the edge of the boundary layer. The index n must be evaluated for the profile to be defined.

Myring [5] gives the displacement area Δ^* of the boundary layer as

$$\Delta^* = \delta^* \left(r + \frac{\delta^*}{2} \cos\alpha\right) \qquad (3)$$

or, assuming the power law velocity profile, as

$$\Delta^* = \frac{r\delta}{(1+n)} + \frac{\delta^2}{2} \frac{\cos\alpha}{(1+2n)} \qquad (4)$$

where r is the body radius and α is the angle between the body surface and the body axis. From the computed data and a knowledge of the body geometry it was possible to evaluate Δ^* from equation (3) and to obtain from equation (4) a quadratic expression in n from which only one reasonable solution could be obtained. A velocity profile in terms of U/U_1 was calculated from which a profile of U/U_o was obtained for comparison with the measurements.

5. RESULTS

5.1 Results for the 6 inch diameter axisymmetric body.

The measured and computed velocity profiles for the 6 inch diameter body are shown in figures 3(a) to (c) for a model location 18 inches into the duct. Transition from a laminar turbulent boundary layer was selected for the computation to occur at 85.5° around the hemispherical nose (measured from the body axis) as for the computations reported previously [1], and this is equivalent to an axial distance, x_t, of approximately 2.8 inches. It should be noted that no attempt has been made to fair the computed boundary layer and potential flow profiles together. The agreement between the computed curves and the measured data points is good, both in terms of profile shape and the magnitude of the velocity ratios which generally differ by less than 3% of the measured value. The pressure coef-

ficients derived from the airspeed measured at the boundary layer edge are shown in figure 3(d) together with the computed values obtained from the potential flow at the body surface. The most significant differences occur at the start of the body taper and are partly due to the variation of potential flow velocity ratio with radial distance leading to values at the boundary layer edge position which are very different from those at the body surface. The similarity of the velocity profiles indicates that the comparison would be improved by recomputing the pressure coefficients using the potential flow velocity at a radial distance equal to that of the boundary layer edge. At other axial positions the potential flow velocity ratio does not vary much with radial distance.

5.2 Results for the 8 inch diameter axisymmetric body.

Three positions of the model in the duct were examined and the measured and computed results are shown in figures 4, 5 and 6. The boundary layer transition position used in the computations was at an angle of 85.5° around the hemispherical nose, as for the 6 inch body computations, and this is equivalent to an axial distance, x_t, of approximately 3.7 inches. Agreement between the computed velocity profiles with the measured data points for the model at 10 inches and 30 inches into the duct (figures 4 and 6) was usually poor, especially in the tail region. However, with the model at 20 inches into the duct (figure 5) the agreement was much better up to about 40 inches along the model beyond which the accuracy of the first order boundary layer computation is expected to be poorer and there may be effects in the actual flow due to the model's tail sting.

Figure 7 shows the variation of the measured and computed boundary layer thicknesses with measurement position and model position. The variation of thicknesses with measurement position is followed closely by the computation although the magnitudes are different, whereas the variation within model position is not computed correctly. It is evident that moving the model forward decreased the boundary layer thickness whereas the computations resulted in increased thickness.

As the actual boundary layer transition position was not determined during the experiment it was thought that the assumed, computation value could be incorrect and that, because of the low turbulence in the wind tunnel, the transition occurred further aft. A number of other positions were selected and a position found at which calculated thicknesses agreed closely with measurements for the model positioned at 30 inches into the duct. Another position was found, slightly forward of the original transition position, which improved the agreement for the model positioned at 20 inches into the duct. A transition position very close to the nose failed to produce useful results and so the agreement for the model at 10 inches was not improved. Figure 8

shows the best agreement with measurements obtained for the three model positions. Further improvement for the model 30 inches into the duct could be made by reducing the interval between the body coordinates used in the computation, thus defining the transition position more precisely.

As mentioned previously, it is not unreasonable to expect the transition to occur further aft than when the models were tested in the 12 inch diameter wind tunnel [1] because that wind tunnel had much more turbulent flow than the Quiet Wind Tunnel which has a turbulence level of 0.2%. It is not clear why the transition position on the model should change with its position in the duct as the computations suggest unless the duct wall boundary layer had an effect or the turbulence levels were significantly different between the cases. The duct wall boundary layer grew to approximtely 0.8 inches thick at the duct exit and is therefore significant. The turbulence level in the flow between the boundary layers was less than 0.13% for all three cases and so is unlikely to have caused any movement of the transition position.

The pressure coefficient variation along the 8 inch body at 20 inches into the duct is shown in figure 9 and is very similar to that of the 6 inch body shown in figure 3(d) and the same comments apply. As the computed pressure coefficients are obtained from the potential flow calculations they are unaffected by changes to the boundary layer transition position.

6. CONCLUSIONS

The comparison of computed and measured boundary layer profiles and thicknesses has shown that very good agreement can be obtained provided a suitable position for the boundary layer transition from laminar to turbulent flow can be chosen for the computation. As no attempt was made to determine the real transition position it is not known if the positions chosen were realistic. They are, however, reasonable positions in terms of transition positions for similar flows over flat plates and spheres. The computations suggest that the transition position moves rearward as the model is moved forward into the duct.

It is evident that, in attempting to simulate a full scale flow field, this computer program can be a valuable guide in selecting the most suitable model and duct configuration, although some preliminary testing may be necessary to establish the boundary layer transition position and possibly change it by using a boundary layer trip device. These and the earlier results have shown that models with a diameter of approximately half the duct diameter can be used in wind tunnel tests without preventing full development of the boundary layer.

G J Cooper (HSO)
ARE/RJE

REFERENCES

1. COOPER, G J. Comparison of Measured and Computed Boundary Layers at the Tail End of an Axisymmetric Body in an Air-Jet. AMTE(N)TM83053, January 1983.

2. HESS, J L and SMITH, A M O. Calculation of Potential Flow about Arbitrary Bodies. Progress in Aeronautical Sciences 8, Pergamon Press 1966.

3. ERITH, M J. Axisymmetric Potential Flow past a Propelled Body in a Semi-Infinite Duct. AMTE(N) TR80103 October 1980.

4. ROSENHEAD, L. (ed) Laminar Boundary Layers, O.U.P. 1983.

5. MYRING, D F. The Profile Drag of Bodies of Revolution in Subsonic Axisymmetric Flow. RAE TR72234, May 1973.

6 INCH DIAMETER BODY		8 INCH DIAMETER BODY	
Axial distance from nose (inches)	Radius (inches)	Axial distance from nose (inches)	Radius (inches)
0.0	0.0	0.0	0.0
0.0370	0.4689	0.0488	0.6260
0.1469	0.9272	0.1961	1.2358
0.3272	1.3618	0.4358	1.8161
0.5728	1.7630	0.7642	2.3512
0.8791	2.1209	1.172	2.8280
1.2370	2.4272	1.6488	3.2358
1.6382	2.6728	2.1839	3.5642
2.0728	2.8531	2.7642	3.8039
2.5311	3.9630	3.3740	3.9512
3.00	3.00	4.00	4.00
26.00	3.00	29.00	4.00
26.25	2.9961	29.25	3.9969
26.50	2.9819	29.50	3.9870
26.75	2.9598	29.75	3.9701
27.00	2.9291	30.00	3.9461
27.50	2.8390	30.50	3.8791
28.00	2.7142	31.00	3.7858
29.00	2.4291	31.50	3.6650
30.00	2.1429	32.00	3.5240
32.00	1.5709	34.00	2.9520
34.00	1.0000	36.00	2.3811
34.50	0.8449	38.00	1.8091
35.00	0.6551	39.00	1.5240
35.25	0.5350	40.00	1.2339
35.50	0.3780	40.50	1.0689
35.65	0.2390	41.00	0.8728
35.75	0.0	41.50	0.6169
		41.90	0.2760
		42.00	0.0

NB Both bodies were mounted on 1.75 inch diameter tail stings.

TABLE 1. SURFACE COORDINATES FOR AXISYMMETRIC BODIES

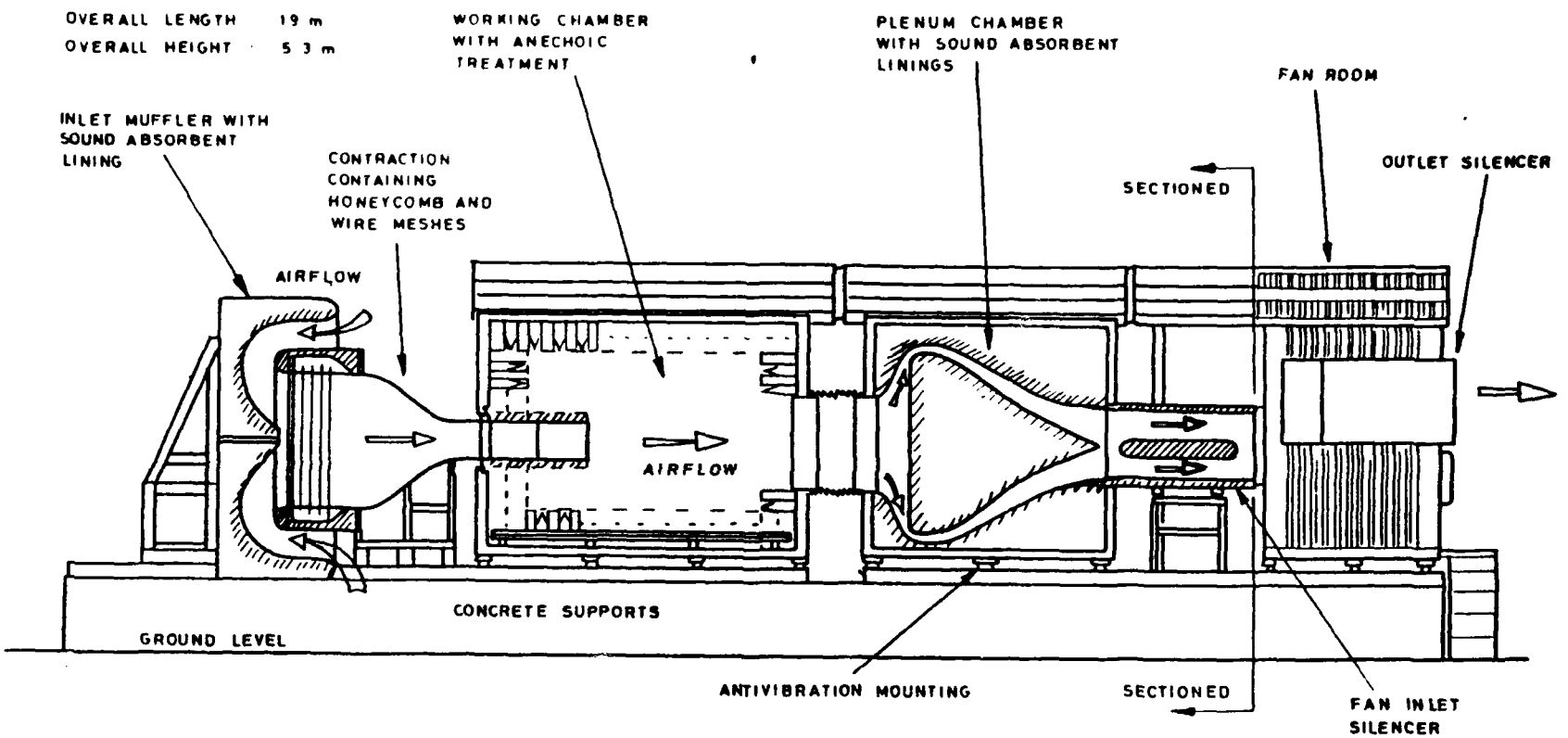

FIG. 1 PARTIALLY SECTIONED ELEVATION OF THE QUIET WIND TUNNEL

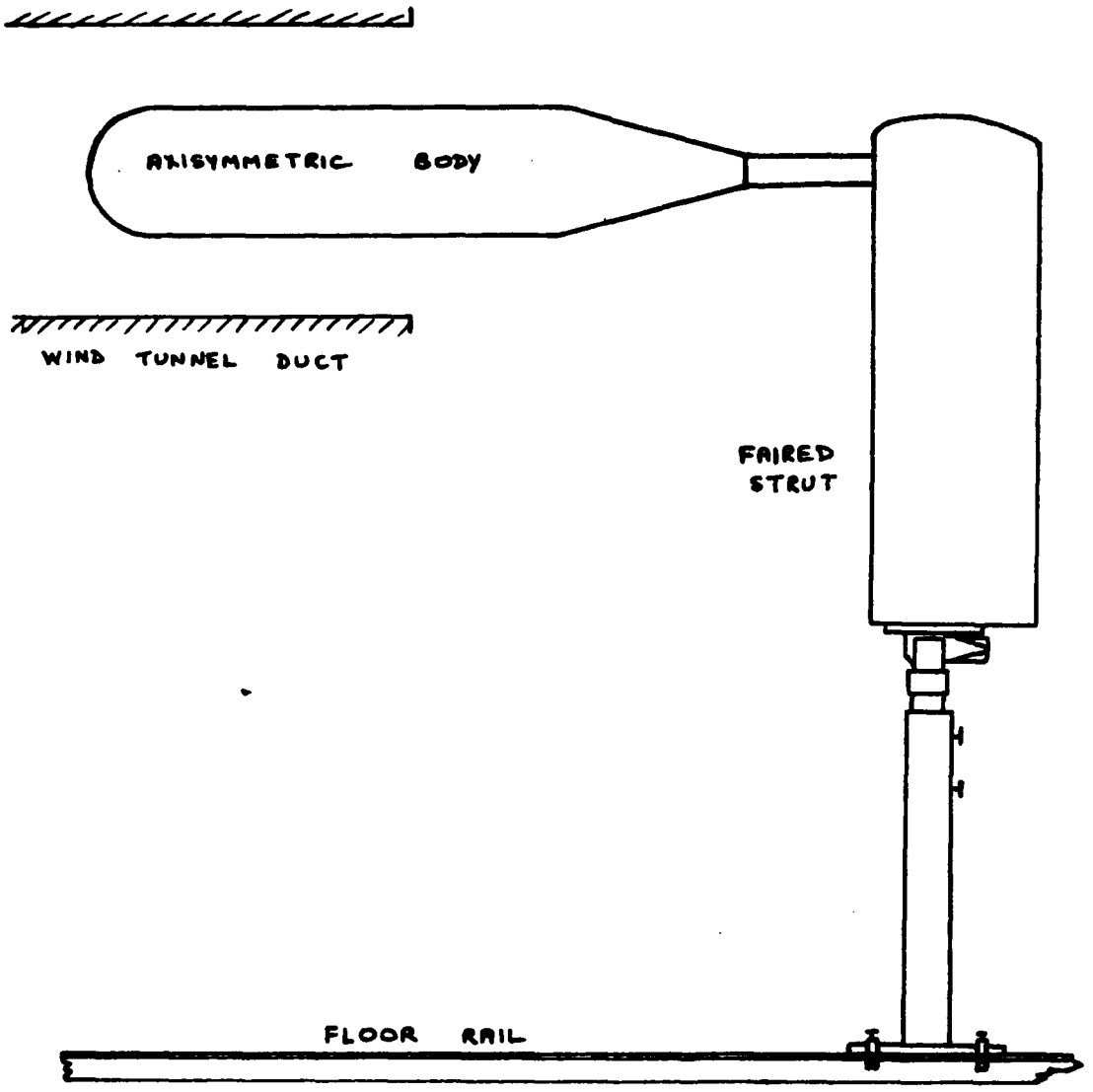

FIG. 2 MODEL MOUNTING

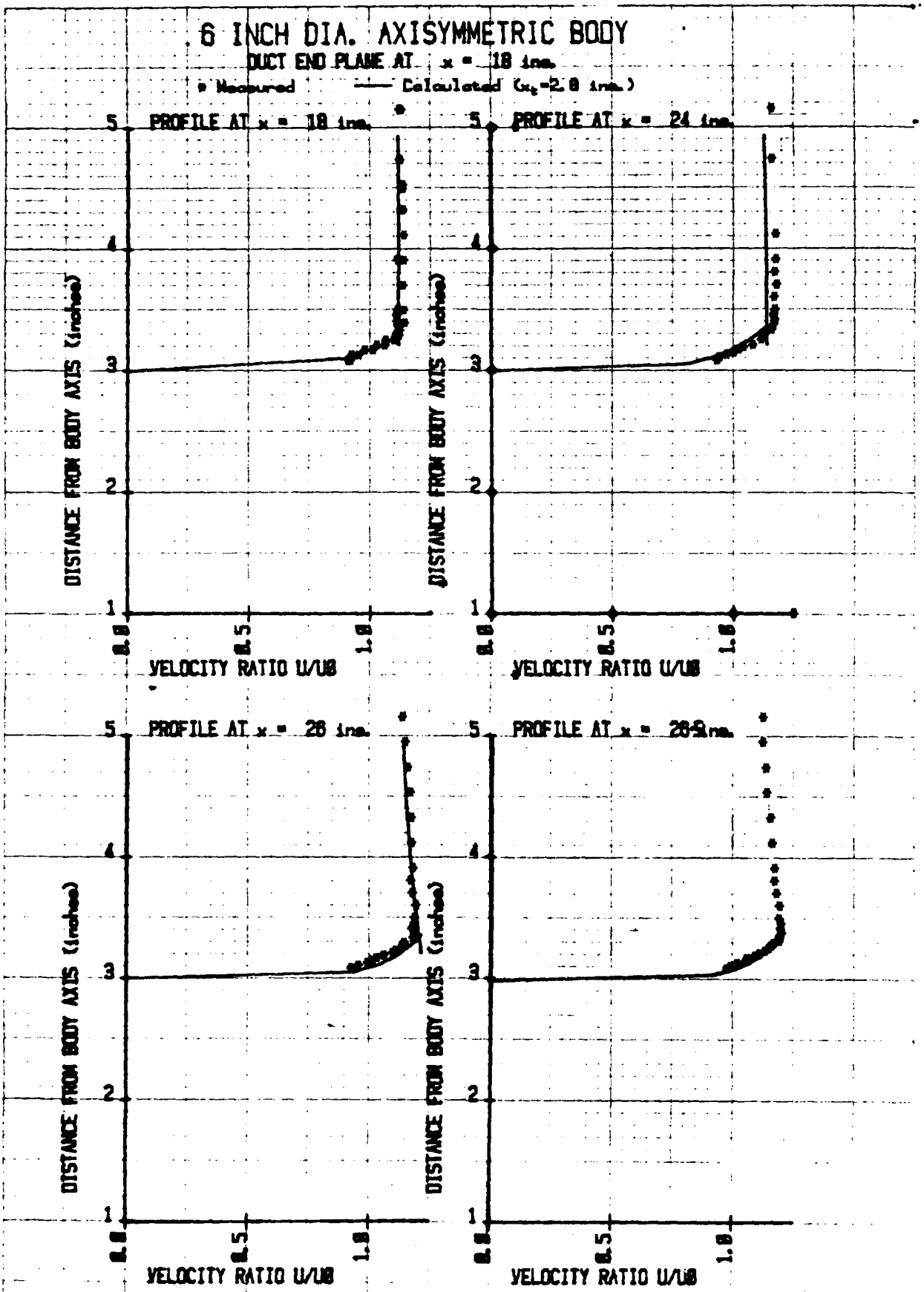

FIG. 3(a) MEASURED AND COMPUTED VELOCITY PROFILES

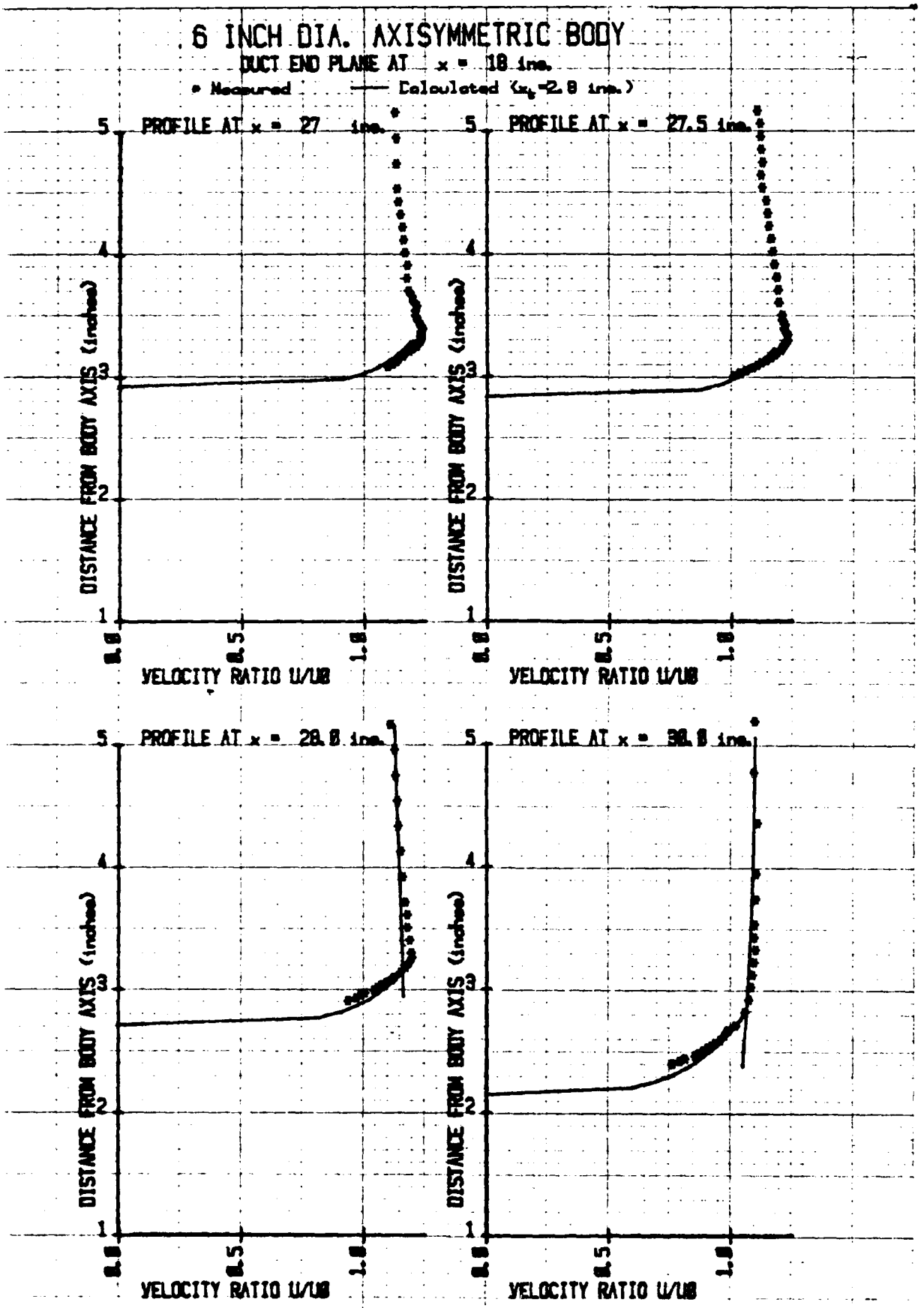

FIG. 3(b) MEASURED AND COMPUTED VELOCITY PROFILES

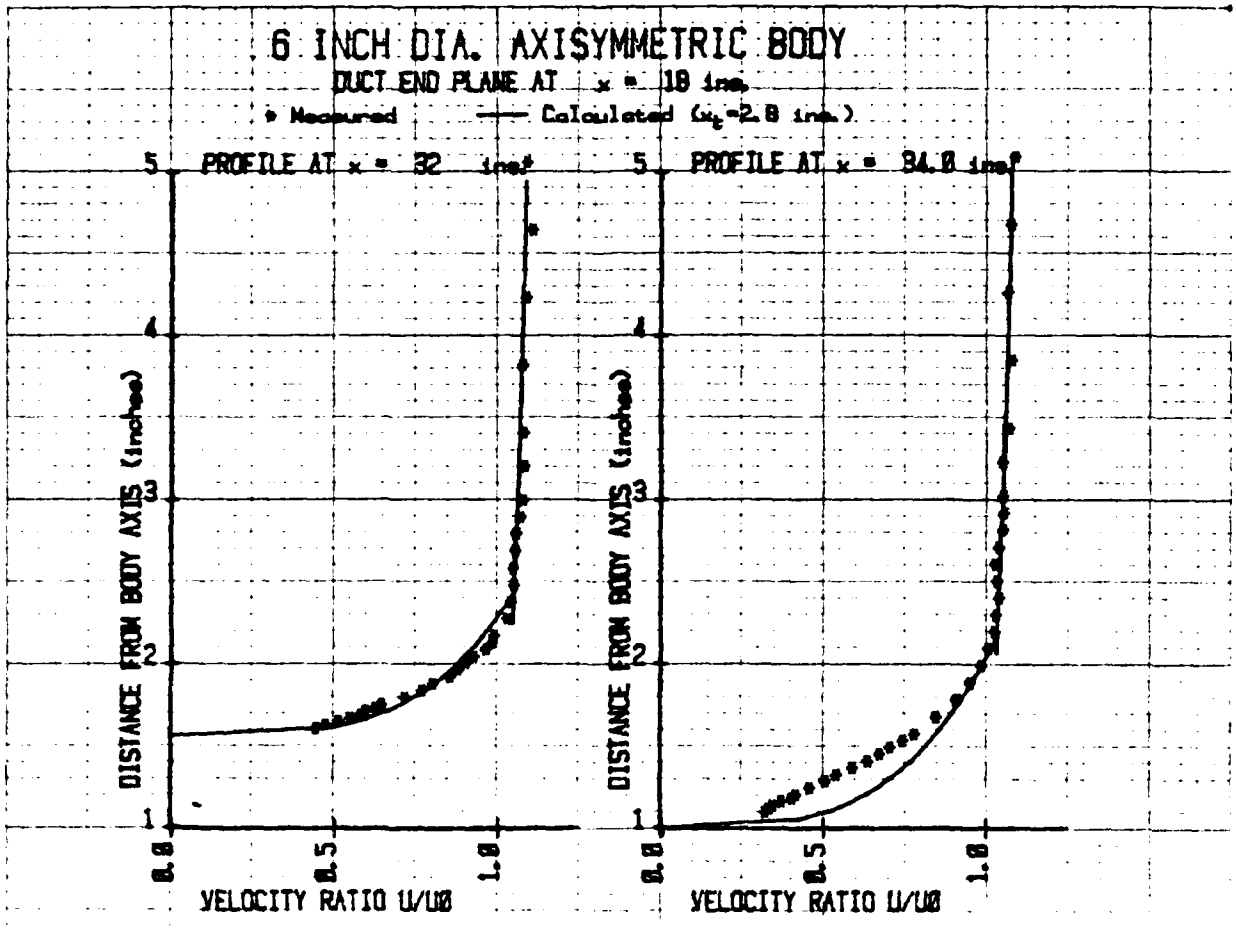

FIG. 3(c) MEASURED AND COMPUTED VELOCITY PROFILES

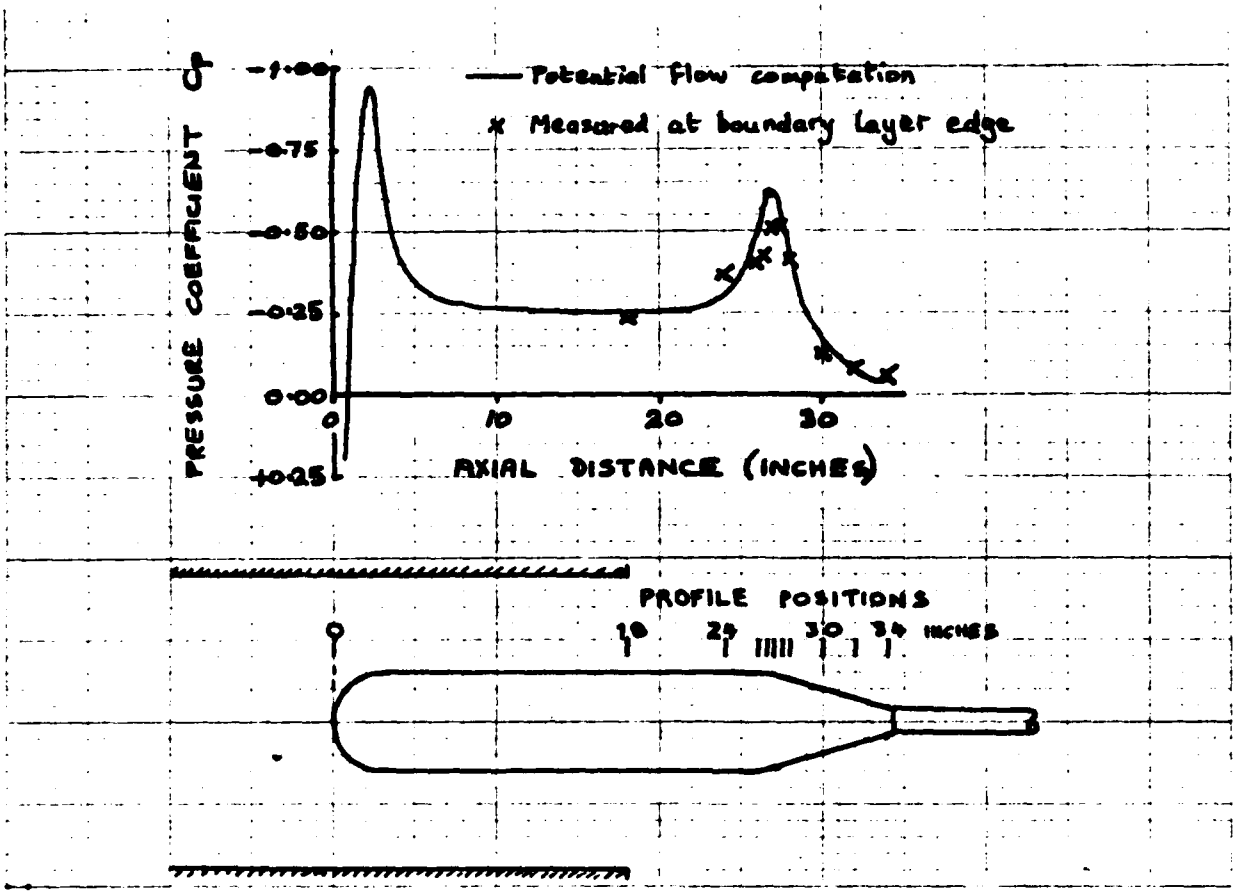

FIG. 3(d) PRESSURE COEFFICIENT DISTRIBUTION

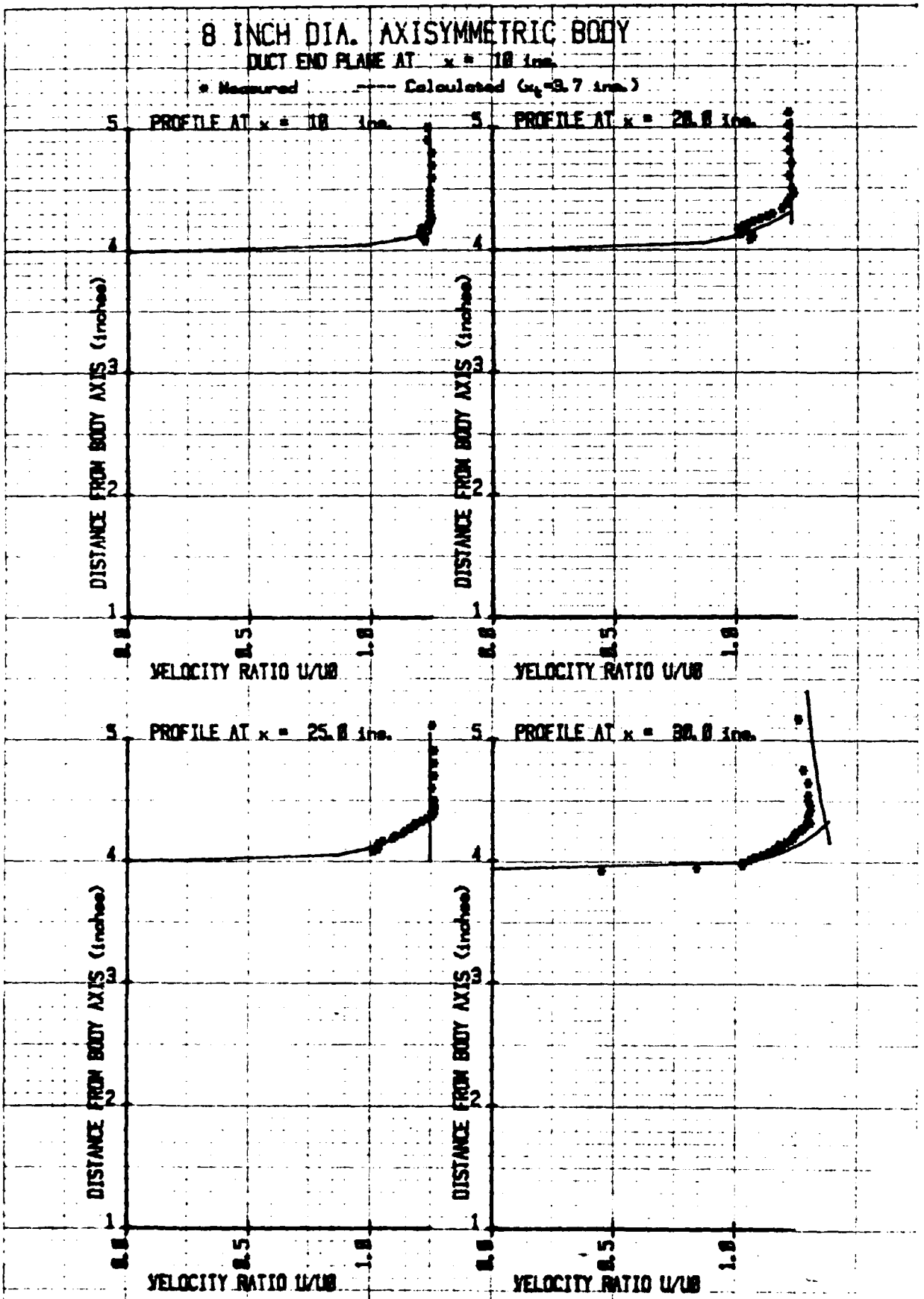

FIG. 4(a) MEASURED AND COMPUTED VELOCITY PROFILES

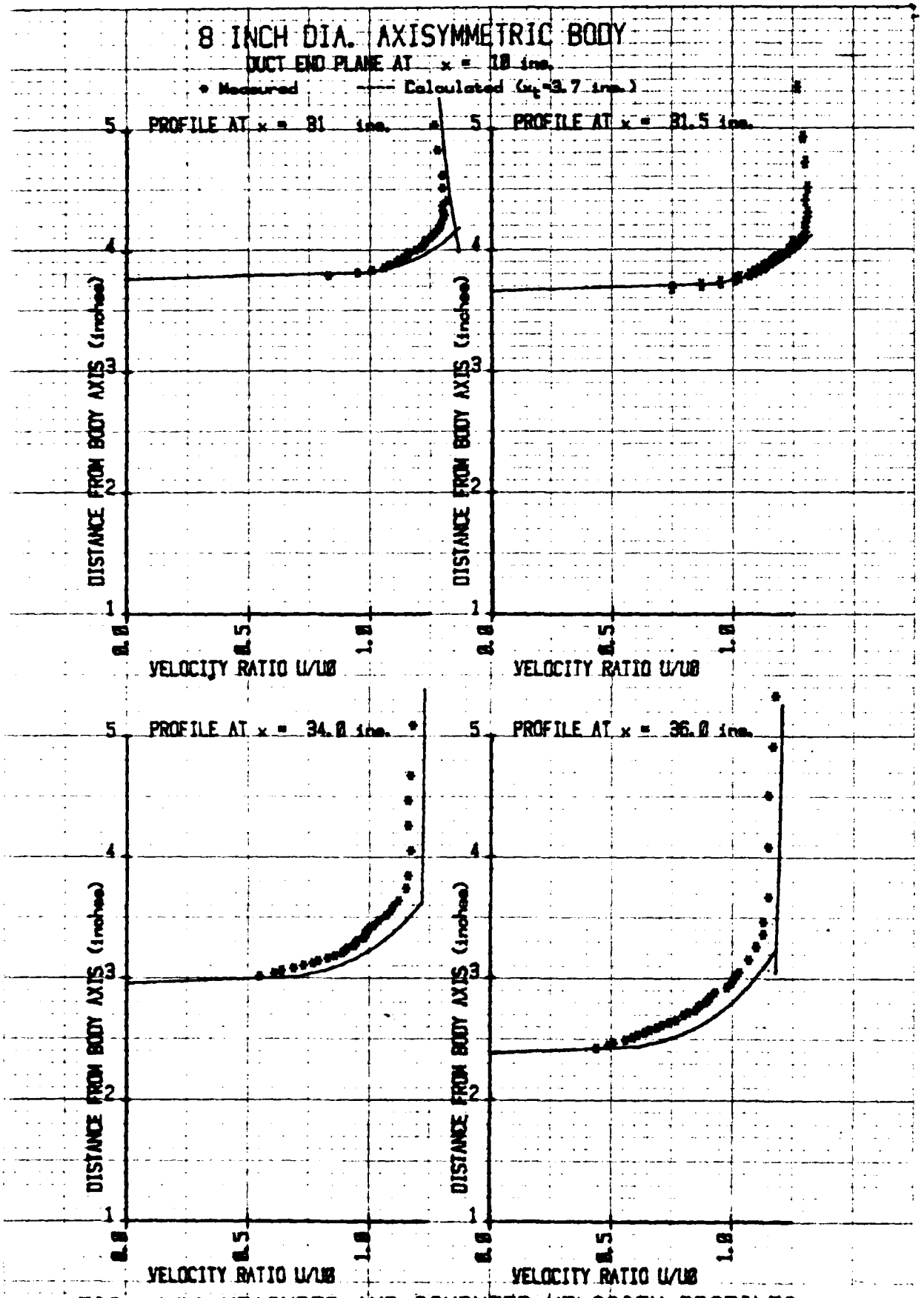

FIG. 4(b) MEASURED AND COMPUTED VELOCITY PROFILES

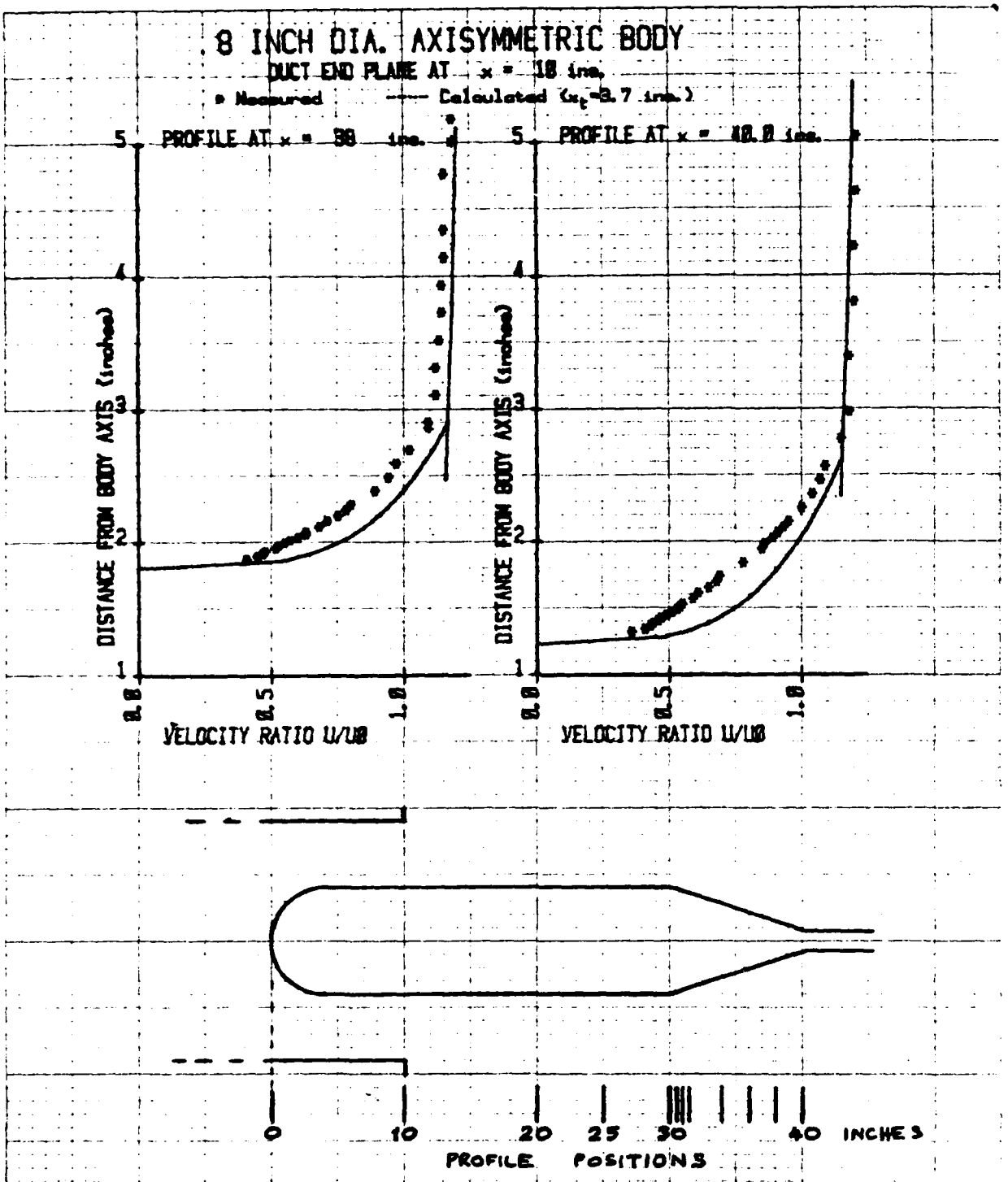

FIG. 4(c) MEASURED AND COMPUTED VELOCITY PROFILES

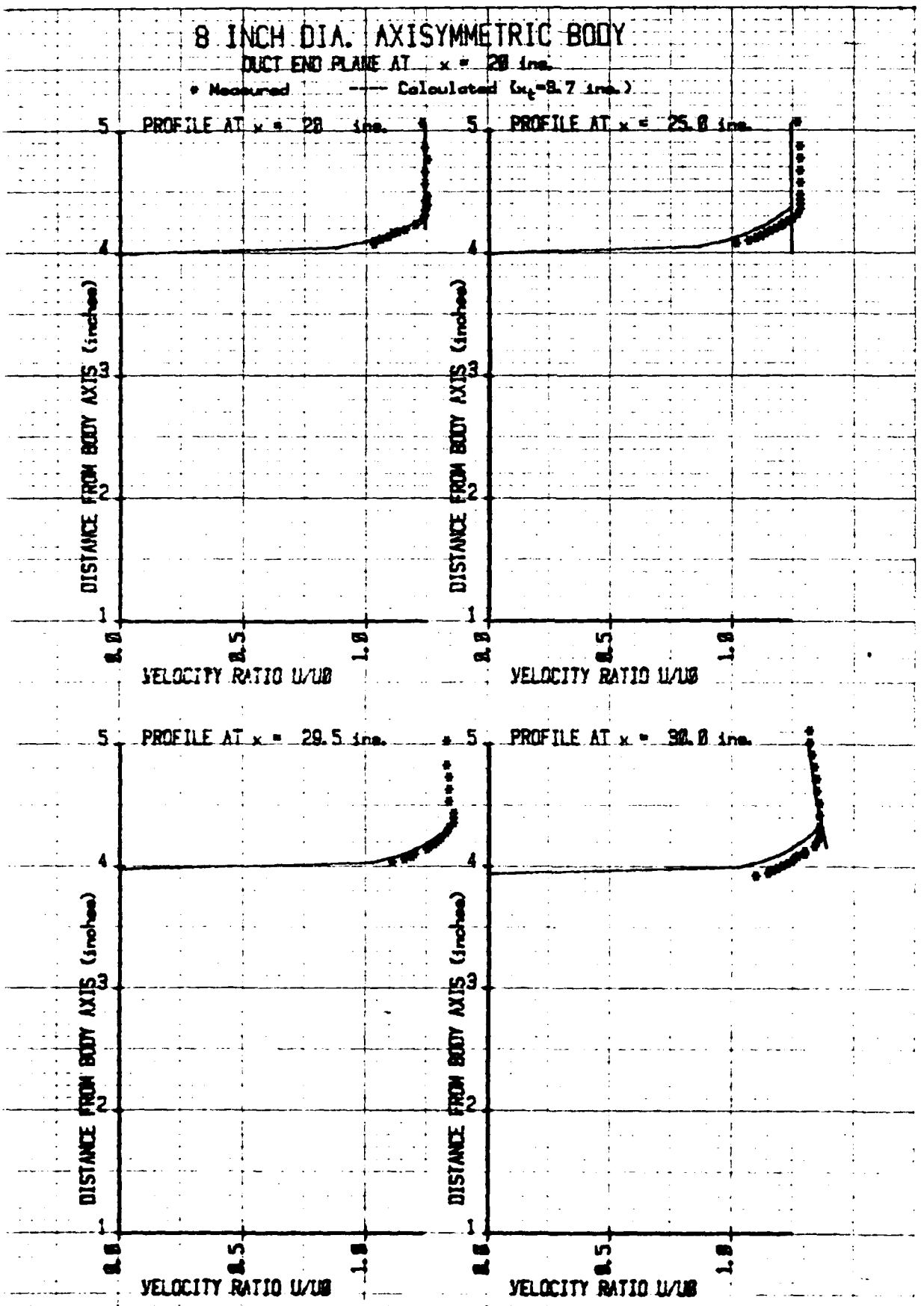

FIG. 5(a) MEASURED AND COMPUTED VELOCITY PROFILES

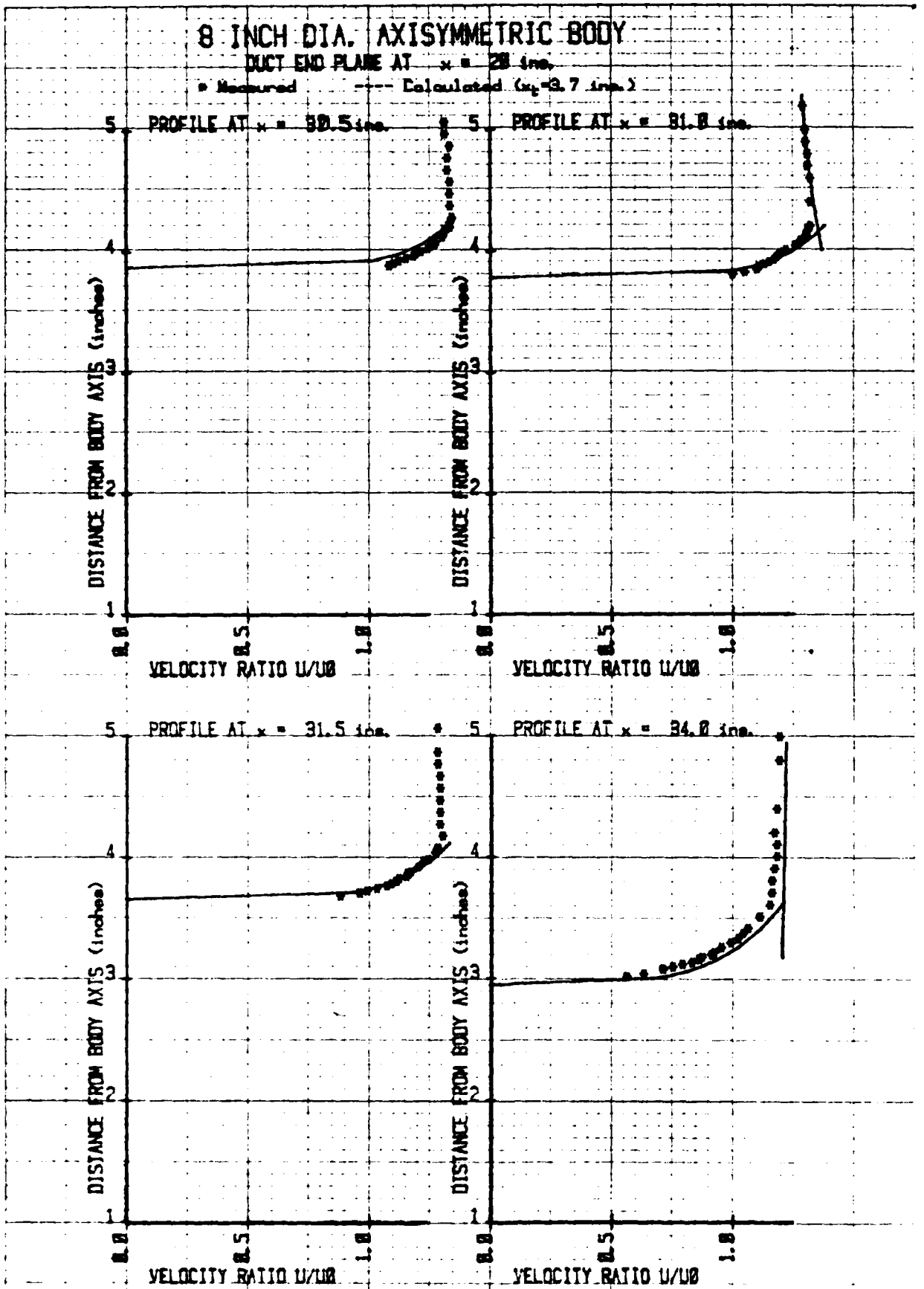

FIG. 5(b) MEASURED AND COMPUTED VELOCITY PROFILES

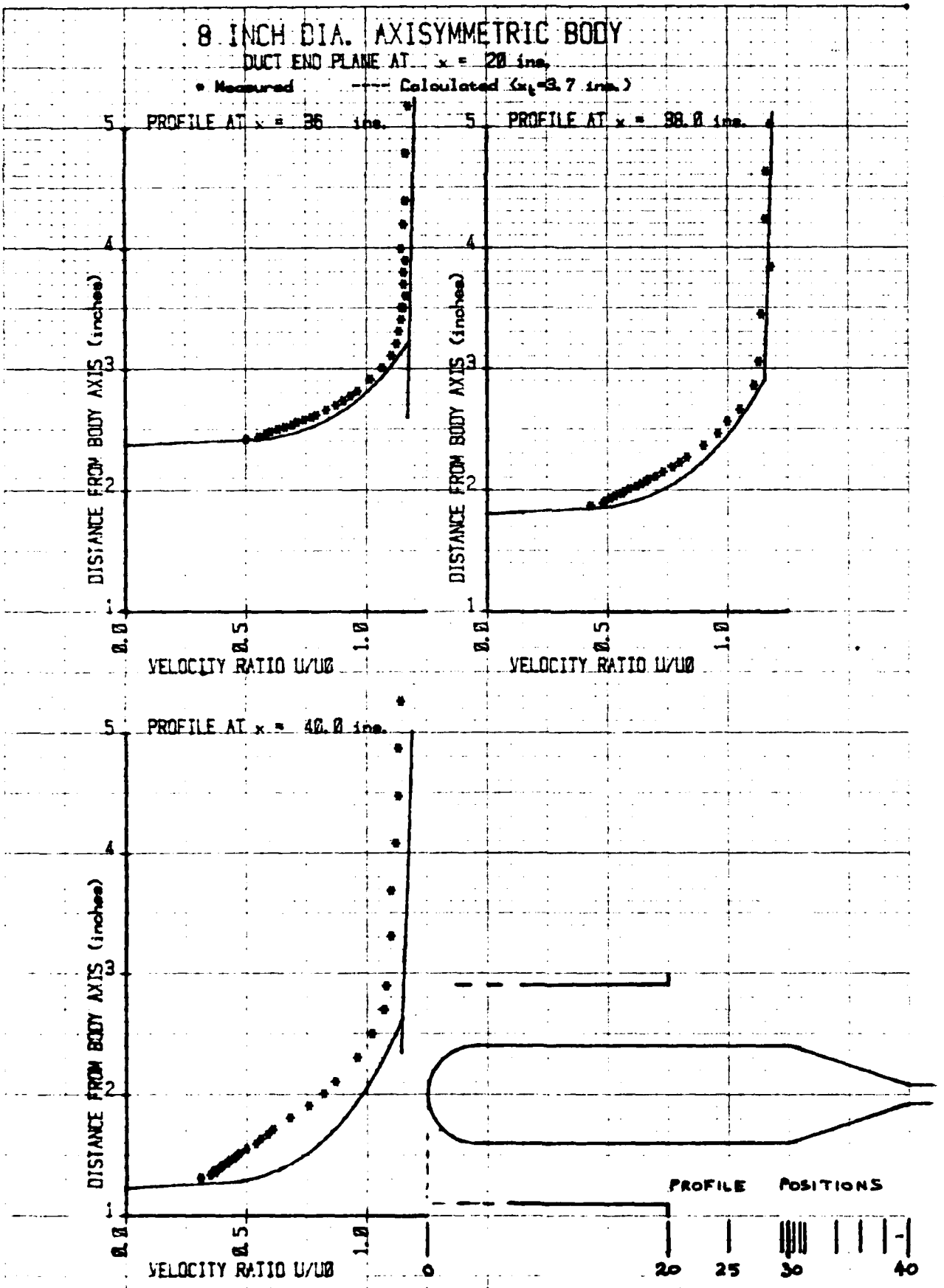

FIG. 5(c) MEASURED AND COMPUTED VELOCITY PROFILES

AMTE (D) TM84003

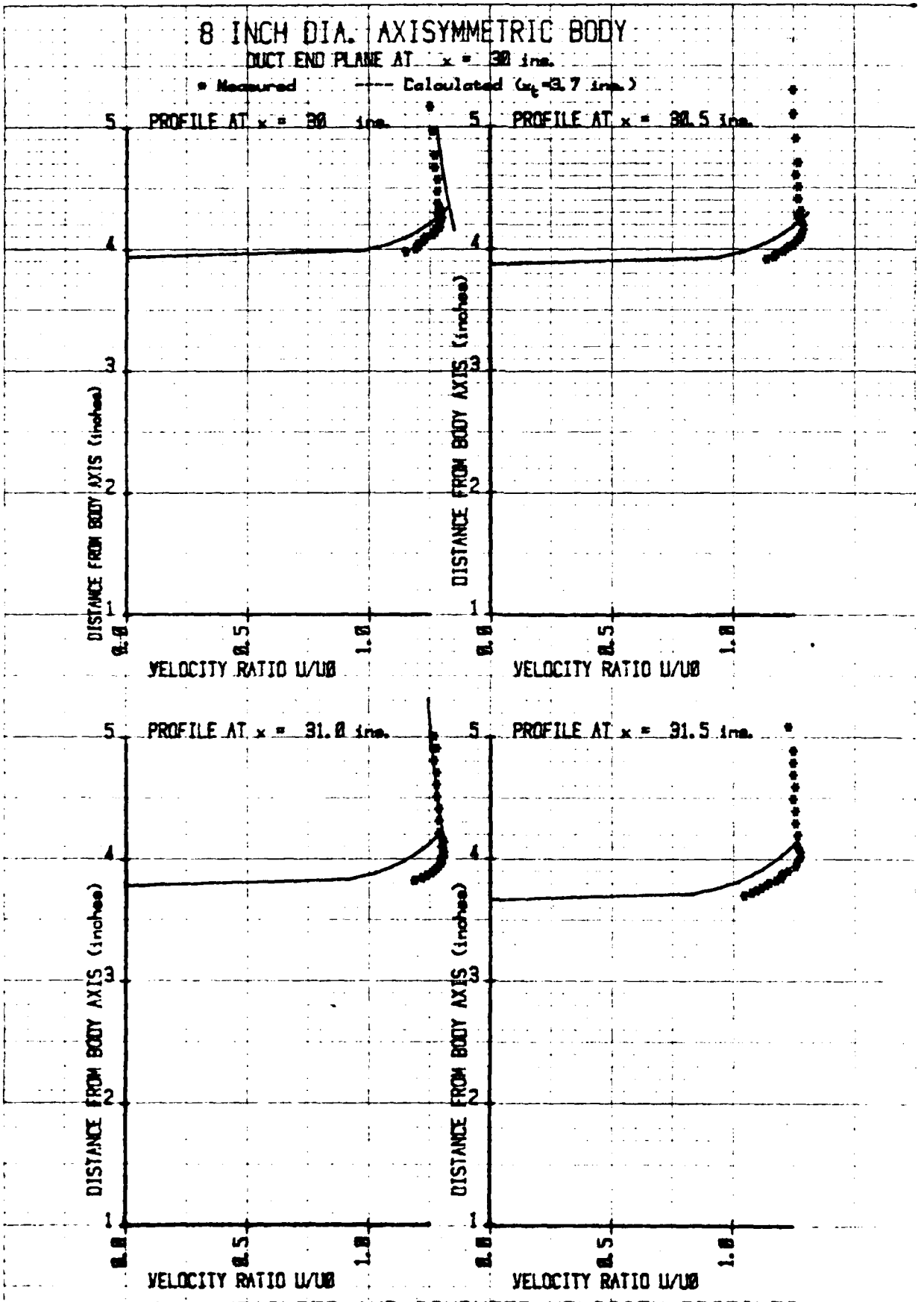

FIG. 6(a) MEASURED AND COMPUTED VELOCITY PROFILES

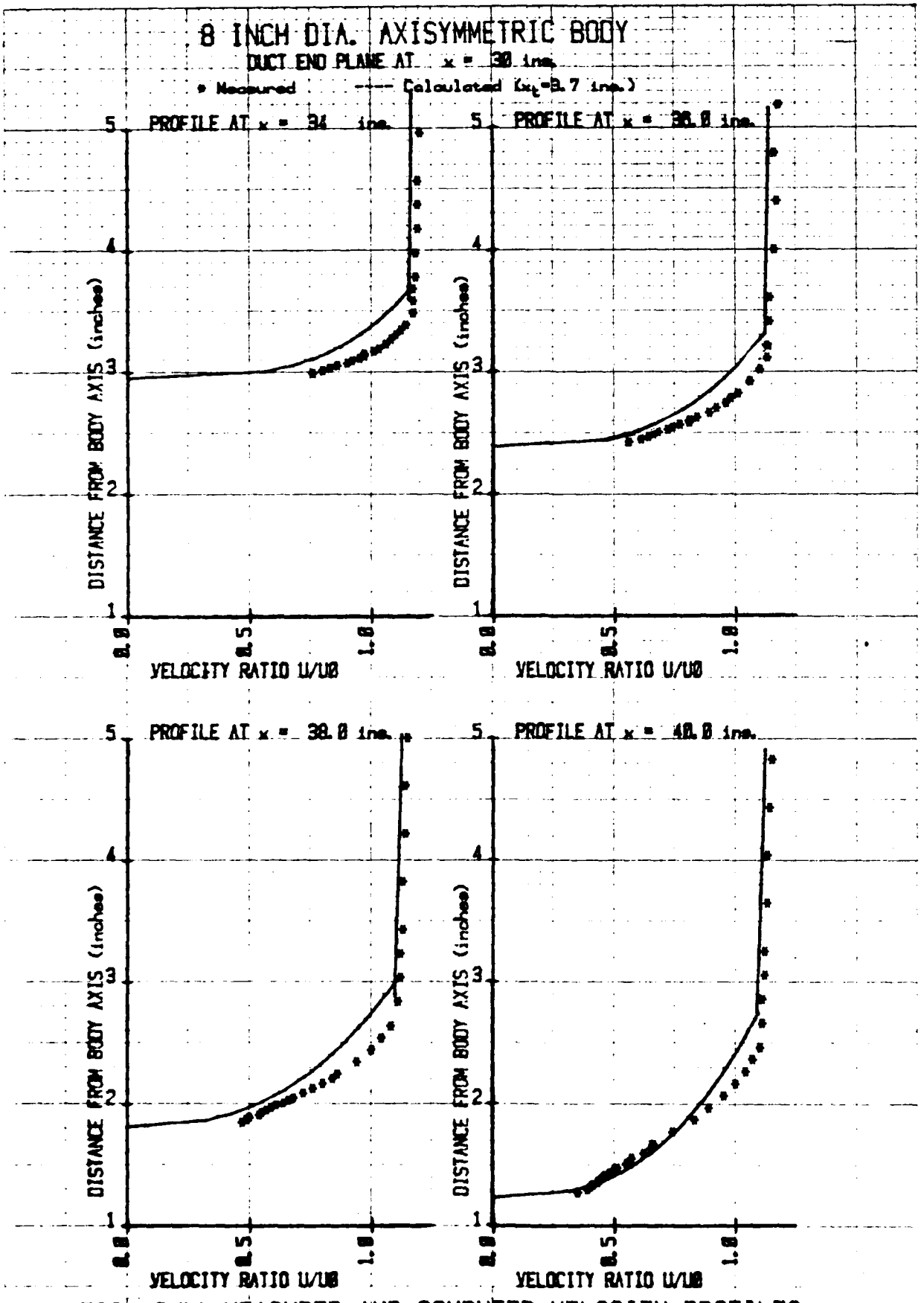

FIG. 6(b) MEASURED AND COMPUTED VELOCITY PROFILES

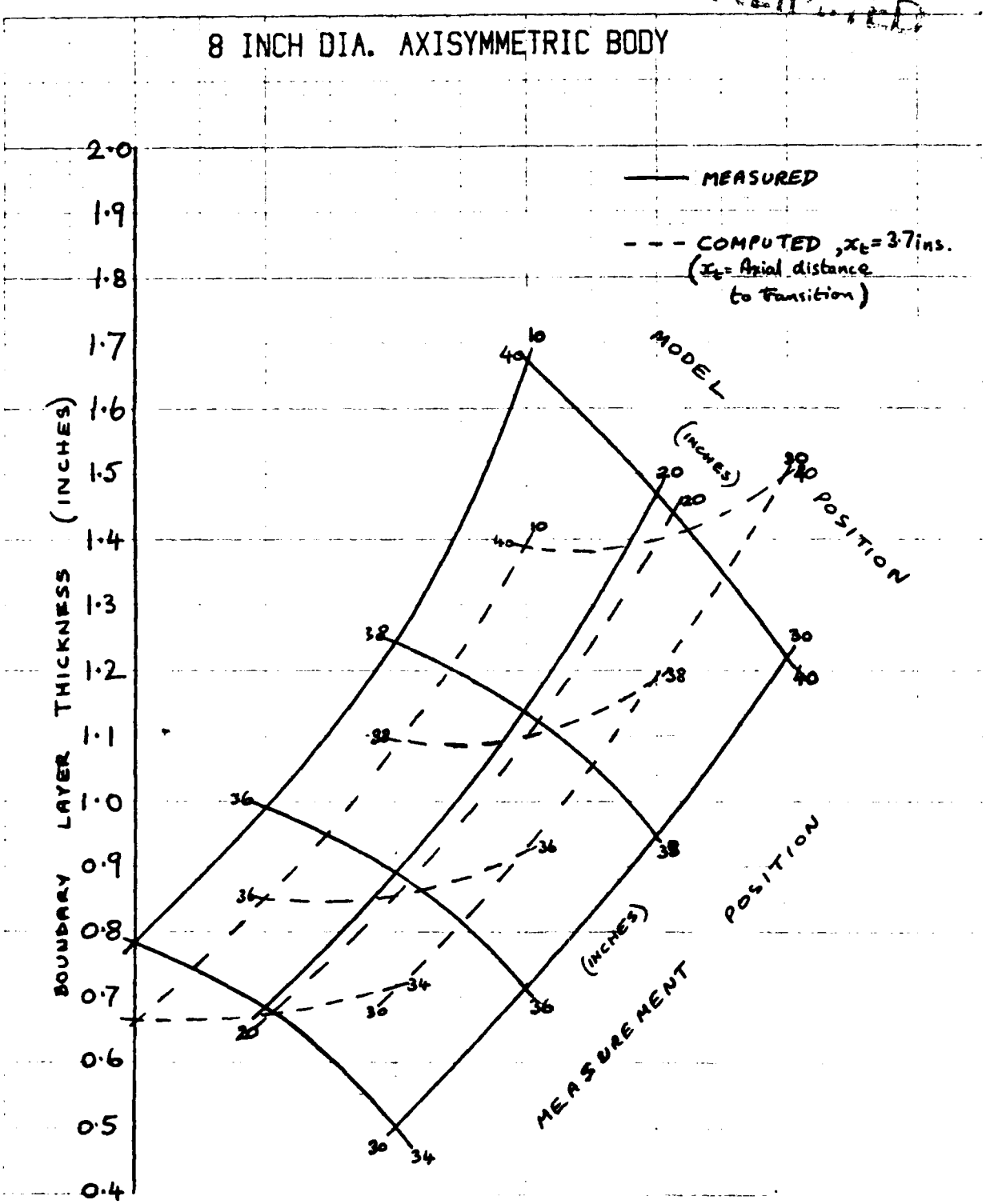

FIG. 7 VARIATION OF BOUNDARY LAYER THICKNESS WITH MODEL POSITION AND MEASUREMENT POSITION

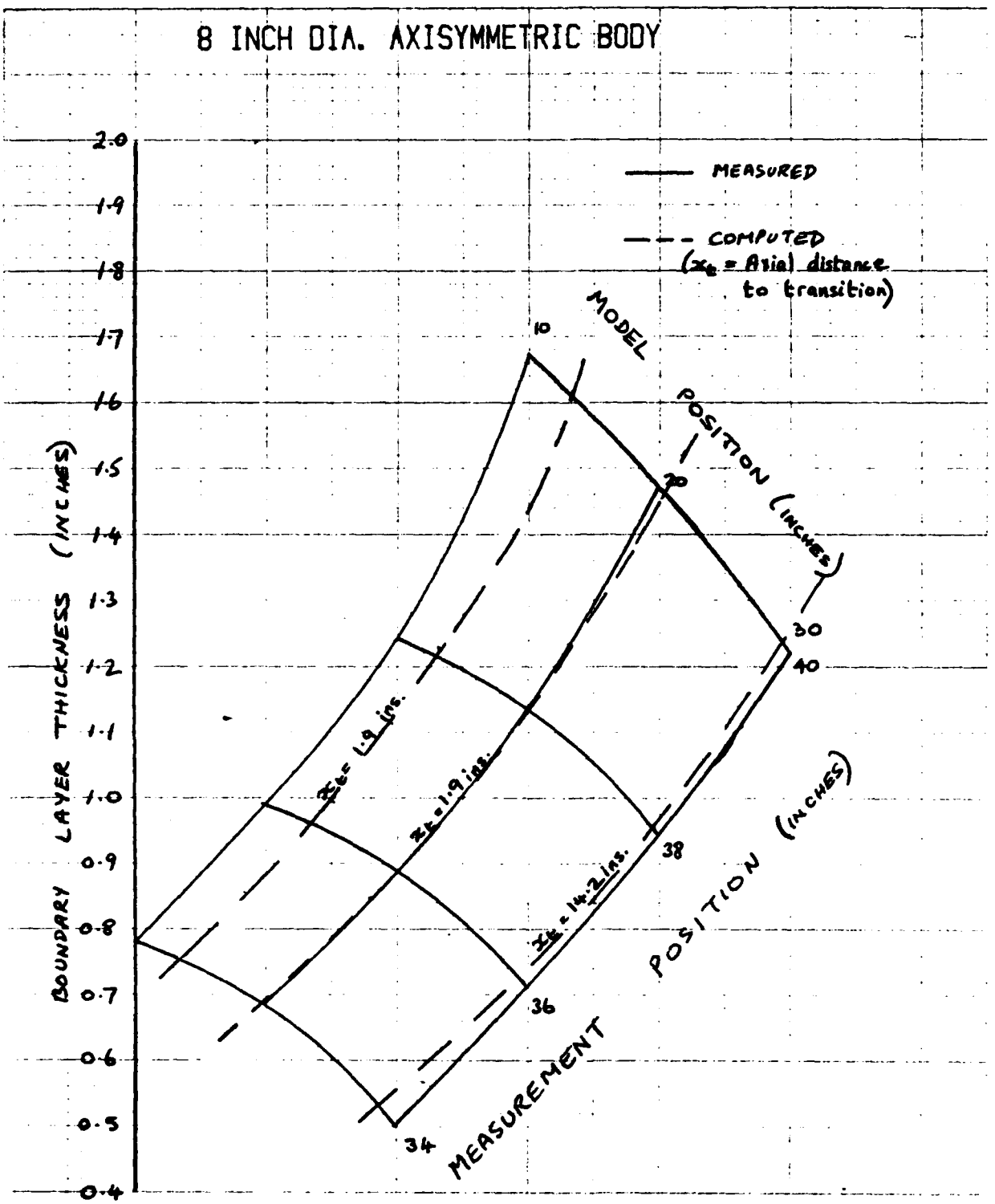

FIG. 8 VARIATION OF BOUNDARY LAYER THICKNESS WITH MODEL POSITION AND MEASUREMENT POSITION

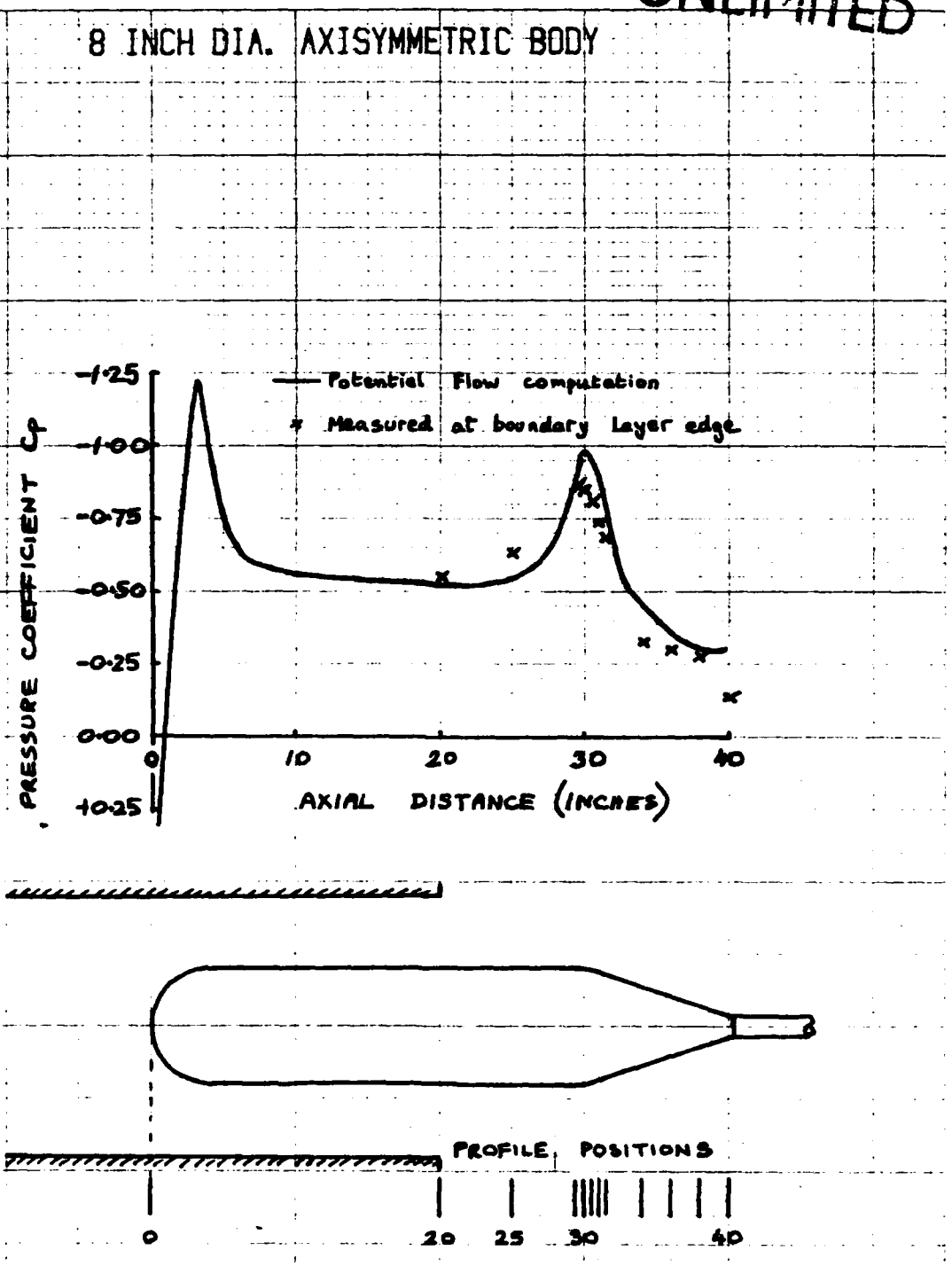

FIG. 9 PRESSURE COEFFICIENT DISTRIBUTION

END

FILMED

3-86

DTIC